

Lateral root morphogenesis is dependent on the mechanical properties of the overlaying tissues

Mikaël Lucas^{a,b}, Kim Kenobi^a, Daniel von Wangenheim^{c,d}, Ute Voß^a, Kamal Swarup^a, Ive De Smet^{a,e}, Daniël Van Damme^{f,g}, Tara Lawrence^a, Benjamin Péret^a, Eric Moscardi^h, Daniel Barbeau^h, Christophe Godin^h, David Saltⁱ, Soazig Guyomarc'h^j, Ernst H. K. Stelzer^c, Alexis Maizel^{d,1}, Laurent Laplace^{b,1}, and Malcolm J. Bennett^{a,1}

^aCentre for Plant Integrative Biology, University of Nottingham, Nottingham LE12 5RD, United Kingdom; ^bInstitut de Recherche pour le Développement, Unité Mixte de Recherche (UMR) Diversité Adaptation et Développement des Plantes (DIADE), 34394 Montpellier Cedex 5, France; ^cBuchmann Institute for Molecular Life Sciences, Goethe University Frankfurt, D-60438 Frankfurt am Main, Germany; ^dCenter for Organismal Studies, University of Heidelberg, D-69120 Heidelberg, Germany; ^eDivision of Plant and Crop Sciences, School of Biosciences, University of Nottingham, Loughborough LE12 5RD, United Kingdom; ^fDepartment of Plant Systems Biology, VIB, B-9052 Gent, Belgium; ^gDepartment of Plant Biotechnology and Bioinformatics, Ghent University, 9052 Gent, Belgium; ^hInstitut National de Recherche en Informatique et Automatique, Virtual Plants team, Unité Mixte de Recherche Amélioration Génétique et Adaptation des Plantes, 34095 Montpellier, France; ⁱInstitute of Biological and Environmental Sciences, University of Aberdeen, Aberdeen AB24 3UU, United Kingdom; and ^jUniversité Montpellier 2, UMR DIADE, Montpellier, France

Edited by Philip N Benfey, Duke University, Durham, NC, and approved January 25, 2013 (received for review June 27, 2012)

In *Arabidopsis*, lateral root primordia (LRPs) originate from pericycle cells located deep within the parental root and have to emerge through endodermal, cortical, and epidermal tissues. These overlaying tissues place biomechanical constraints on the LRPs that are likely to impact their morphogenesis. This study probes the interplay between the patterns of cell division, organ shape, and overlaying tissues on LRP morphogenesis by exploiting recent advances in live plant cell imaging and image analysis. Our 3D/4D image analysis revealed that early stage LRPs exhibit tangential divisions that create a ring of cells corraling a population of rapidly dividing cells at its center. The patterns of division in the latter population of cells during LRP morphogenesis are not stereotypical. In contrast, statistical analysis demonstrated that the shape of new LRPs is highly conserved. We tested the relative importance of cell division pattern versus overlaying tissues on LRP morphogenesis using mutant and transgenic approaches. The double mutant *aurora1 (aur1) aur2* disrupts the pattern of LRP cell divisions and impacts its growth dynamics, yet the new organ's dome shape remains normal. In contrast, manipulating the properties of overlaying tissues disrupted LRP morphogenesis. We conclude that the interaction with overlaying tissues, rather than the precise pattern of divisions, is most important for LRP morphogenesis and optimizes the process of lateral root emergence.

lateral root development | plant morphogenesis | biomechanical regulation | statistical shape analysis | *Arabidopsis thaliana*

In contrast to animals, only the basic blueprint of the plant body plan is laid out during embryogenesis. Instead, the majority of plant organs are formed postembryonically. In some instances, organ formation can occur deep within another organ, as is the case for lateral roots (1, 2). In addition, plant cells are constrained by rigid walls; hence, cell migration cannot occur. Instead, plant morphogenesis relies on two mechanisms: oriented cell division and anisotropic growth (3, 4). For example, during embryogenesis, cells exhibit a highly synchronized program of expansion and division (5). How cell division, cell shape, and overlaying tissues interact during plant organ morphogenesis is currently unclear.

Lateral roots are derived from cell division events deep within the primary root (1, 2). Pairs of pericycle cells in several adjacent files undergo a series of asymmetric formative divisions (reviewed in ref. 6). These periclinal (parallel) and anticlinal (perpendicular) divisions give birth to a lateral root primordium (LRP) that will develop further into a lateral root comprising a new root meristem. LRP formation in *Arabidopsis* was first described in a pioneering study 14 years ago (7) that proposed a seven-stage taxonomy of LRP development on the basis of 2D observations of cell layer numbers that still forms the basis of all studies describing LRP development in *Arabidopsis*.

Recent advances in live biological imaging and image analysis (8, 9) now make it possible to address how *Arabidopsis* LRPs are built in three and four dimensions. Here, we report how 3D/4D image reconstruction reveals important divisions that are responsible for the transition from a bilateral to a radial symmetry of the LRP. Surprisingly, our study indicates that the pattern of cell division in LRP formation is much less precise and more variable than presumed. We present genetic evidence confirming that disrupting the pattern of cell divisions had only a minor effect on LRP shape, whereas it affected the dynamics of its growth. In contrast, manipulating the properties of overlaying tissues disrupted LRP morphogenesis. We conclude that the interaction with overlaying tissues, rather than the precise pattern of divisions, is most important for LRP morphogenesis.

Results

Three- and Four-Dimensional Image Analysis Reveals That LRPs Undergo Radialization During Emergence. In *Arabidopsis* LRPs originate from pairs of pericycle cells positioned opposite the root xylem pole (10). At the onset of lateral root initiation, these cells undergo asymmetric division, giving rise to two abutting short cells flanked by two longer daughter cells (Fig. 1A). The longer daughter cells undergo several further rounds of asymmetric cell division to create a stage I primordium composed of a core of short daughter cells flanked by the remaining longer daughter cells (11). It is often overlooked that LRPs are derived from not one but three pairs of pericycle cells originating from three adjacent cell files, which undergo the same pattern of asymmetric cell divisions (12) (Fig. 1A). However, it remains unclear how this structure with a bilateral symmetry can give rise to the radially organized 3D LRP.

To characterize the development of LRP 3D/4D shape, we initially used confocal microscopy to monitor primordia expressing pAUX1::AUX1-YFP (13) or a ubiquitously expressed plasma membrane marker pUB10::WAVE131-YFP (14). We collected z-stacks for several hundred LRPs (ranging from stage I to VI) to precisely document the orientation of cell divisions in 3D (see Fig. S1 for example images). Our confocal image reconstructions revealed that, in addition to previously reported anticlinal and

Author contributions: I.D.S., A.M., L.L., and M.J.B. designed research; M.L., D.v.W., U.V., K.S., D.S., and S.G. performed research; D.v.W., D.V.D., T.L., B.P., E.M., D.B., C.G., S.G., E.H.K.S., and A.M. contributed new reagents/analytic tools; M.L., K.K., D.v.W., U.V., K.S., E.M., D.B., C.G., A.M., L.L., and M.J.B. analyzed data; and M.L., I.D.S., A.M., L.L., and M.J.B. wrote the paper.

The authors declare no conflict of interest.

This article is a PNAS Direct Submission.

¹To whom correspondence may be addressed. E-mail: malcolm.bennett@nottingham.ac.uk, alexis.maizel@cos.uni-heidelberg.de, or Laurent.Laplace@ird.fr.

This article contains supporting information online at www.pnas.org/lookup/suppl/doi:10.1073/pnas.1210807110/-DCSupplemental.

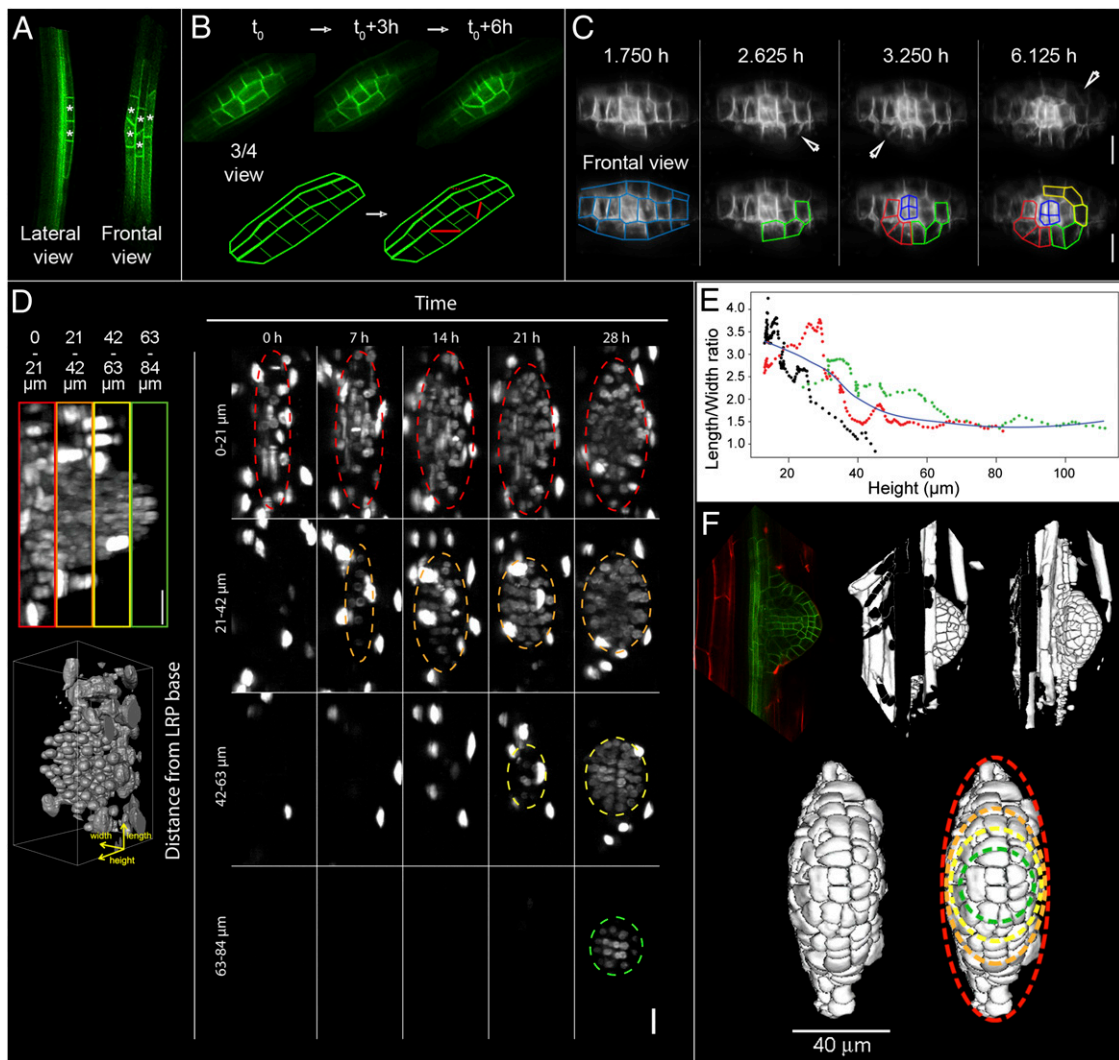


Fig. 1. *Arabidopsis* LRP undergoes radialization during growth. (A) Lateral and frontal view of stage I LRP. Small cells resulting from the first round of asymmetric cell divisions are marked by a white star. (B) Tangential cell divisions during LRP development. (Upper row) Confocal imaging of AUX1-YFP marked LRP, 3/4 frontal view. (Lower row) Schematic representation of the symmetry breaking tangential division events allowing for establishment of radial symmetry. A stack of 180 images at 0.5 μm z-spacing was collected every 1.5 h. (C) Tangential and radial cell divisions during LRP development. (Upper row) Frontal view of light-sheet imaging of a LRP that stably expresses pPIN1:PIN1-GFP. (Lower row) Schematic representation of the constitution of circular buttresses by the tangential and radial cell divisions. Arrowheads highlight the tangential divisions. A stack of images were collected every 7.5 min (scale bar, 20 μm). (D) Light-sheet imaging of a LRP that stably express pUBI10:H2B-RFP. Maximum-intensity projections of four sections located at the indicated distance from the LRP base at the indicated time points are shown. The dashed lines delineate the primordium. The primordium is observed from the top and growing toward the observer (frontal view). In the inset (Left), a side view of the primordium presenting the position of the four sections, color coded, is presented as well as a 3D reconstruction depicting the three axes defined: length is parallel to shootward-rootward axis, width perpendicular to length, and height extends from the base of the primordium away from the main root. A stack of 233 planes each at a 1.29 μm z-spacing was recorded every 15 min for 29 h (scale bar, 20 μm). (E) Development of the L-W ratio according to height for three individual LRPs from light-sheet imaging (D). The L-W ratio was measured at a constant distance from the tip of the LRP (15 μm) and plotted for three independent plants (red, black, and green dots) as a function of the LRP height. The blue line is a Lowess fit of the three individual measurements. (F) 3D reconstruction of LRP from confocal z-stack images. (Upper row) Confocal z-stack at 0.5 μm z-spacing of marked LRPs expressing pAUX1:AUX1-YFP and counterstained with propidium iodide (Left) were treated according to the reconstruction protocol described by ref. 8 to generate 3D reconstruction. (Right; Movies S1 and S2) Spatial analysis of the reconstructed structure reveals a global elliptical profile for developing primordia, as delineated by the colored dashed lines in the bottom row. (Lower row) Isolated frontal view of the reconstructed LRP (Left). Colored outlines (Right) highlight the parts of the LRP corresponding to those observed in light-sheet microscopy (D). Primordium was imaged as a stack of 100 images at 0.5 μm z-spacing.

periclinal divisions, daughter cells flanking the central file underwent division along a tangential plane (Fig. 1B). To independently validate our observations, we used light sheet fluorescence (LSF) microscopy to noninvasively image these tangential divisions (9). LSF microscopy was used to monitor early stage primordia expressing the plasma membrane marker pPIN1:PIN1-GFP (15). Short daughter cells derived from the flanking pairs of pericycle founder cells were clearly observed to undergo either tangential or radial divisions, whereas daughter cells derived from the central pair of pericycle founder cells continued to divide in

anticlinal and periclinal planes (Fig. 1C). Cells undergoing these tangential or radial divisions appeared to “corral” the central bulk of small dividing daughter cells. Such a cellular arrangement was likely to function to buttress the flanks of the LRP to underpin the transition from bilateral to a radial structure.

To ascertain and quantify the radialisation of LRP shape, we followed in wild type plants [Columbia-0 (Col-0)] ubiquitously expressing the RFP marker fused to Histone 2B (H2B-RFP) and in 3D the growth of the LRP over 30 h (from initiation to emergence). Up to 28 h after initiation, the base of the primordium

exhibited an ellipsoid shape (Fig. 1D). LRPs become progressively rounder near their tips as they grew past the cortex and epidermis (Fig. 1D and Movie S1). To quantify this transition, we measured the height, length, and width of the LRP at a fixed distance (15 μm) from the LRP tip and plotted the length–width (L–W) ratio as a function of height for three independent primordia (Fig. 1E). The L–W ratio decreased as the primordia grew, with a steep decline around a height of 40 μm corresponding roughly to the distance between the pericycle and cortex, confirming our observations. An analysis of the hourly growth rate revealed preferential growth along the height (away from the primary root) and width (perpendicular to the primary root) axis of the LRP (Fig. S2). The ellipse-to-round transition of the LRP therefore resulted from the expansion along the width axis.

To reconstruct a 3D surface view of the LRP shape, we used image analysis software (8) to integrate confocal z-stacks of LRP at selected stages (Movies S2 and S3). These data were used for an in-depth investigation of LRP morphogenesis in 3D up to the acquisition of meristematic identity. Light sheet and confocal image reconstruction suggested that although emerged lateral roots adopted a cylindrical shape near their tip, during emergence LRPs form an ellipsoid 3D shape (Fig. 1D and F). Such a structure would be ideally shaped to push between cells in overlaying tissues to facilitate organ emergence.

Pattern of Cell Divisions During LRP Development Is Not Stereotypical.

We next explored the patterns of cell division required to build LRP. The LRP atlas collected using confocal microscopy (see Fig. S1 for example images) was analyzed to reveal these patterns of divisions. Analysis of the number of cells in the centermost (median; Fig. 2A) optical plane of developing LRPs revealed that it is highly variable between different LRPs at a given stage (Fig. 2B), in accordance to the observed variable tissue structure of individual LRPs (Fig. S1). In contrast, the variation of cell numbers estimated within optical slices was found to be low along the z-direction above and below the median optical slices of a given LRP (Fig. S3). This observation is consistent with clonal analysis experiments that concluded that the majority of cells making up LRP originate from the central of three pairs of pericycle cells (12).

While the number of cells in the median optical slice in a population of LRPs appears to be a linear function of the developmental stages of these LRPs, each individual LRP can pass through its developmental stages with markedly different numbers of cells from other LRPs (Fig. 2B). This indicates that the global rate of cell division is constant throughout LRP morphogenesis. This was confirmed by analysis of the total number of cell nuclei of a LRP observed from stage I to VII using LSF microscopy. The total number of cells making up a given stage, scored according to the number of layers present as defined by Malamy and Benfey (7), varied from one- to twofold (Fig. 2C).

Our observation that two consecutive developmental stages may have a similar number of cells (Fig. 2B) suggests that LRP morphogenesis is not a stereotypical sequence leading from one stage to the next. If this were the case, then the passage from one stage to the next would always occur after the same number of cell divisions, and there could be no overlap between the ranges of cell number for each stage. To directly test whether or not LRPs follow stereotyped developmental paths from one stage to the next, we analyzed the developmental time series of individual LRPs (Fig. 2D and Fig. S4). Sequences of cell divisions appeared to occur differently between distinct LRPs (Fig. S4). While the rate of cell division was similar between distinct LRPs, their respective developmental sequences diverged greatly, with LRPs passing through the same developmental stage containing markedly different numbers of cells (Fig. 2D). We conclude that although the progression in terms of number of layers, which defines the stage classification, is one of the key invariants in LRP development, there is no unique sequence of formative cell divisions

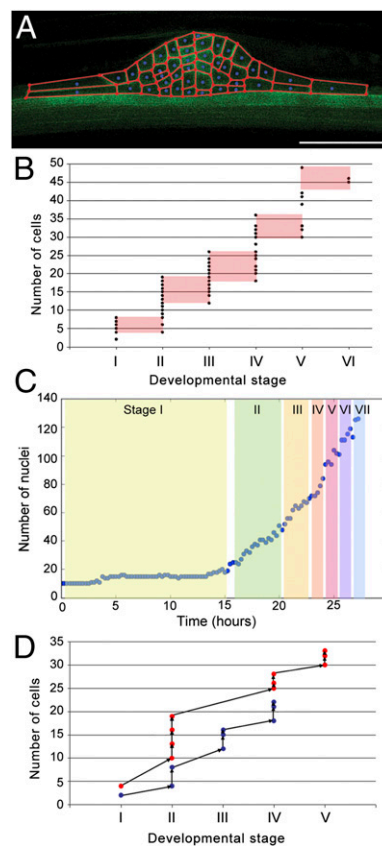


Fig. 2. The program of cell divisions during LRP development is not stereotypical. (A) The internal structure of LRPs was extracted from the median optical slice of confocal z-stacks of primordia that stably express pAUX1:AUX1-YFP. Primordia were imaged as stacks of 150 images at 0.5 μm z-spacing (scale bar, 50 μm). (B) Number of cells in LRP median slices ($n = 117$) as a function of developmental stage. Overlaps in number of cells between stages are highlighted in red. (C) Number of cell nuclei of a developing LRP taken from one of the light-sheet microscopy time series shown in Fig. 1C. For each time point, the LRP median plane was examined to score the developmental stage according to Malamy and Benfey (7). (D) Developmental paths of two distinct LRP (red or blue dots). Time series confocal imaging was used to track the number of cells in LRP median optical slice through time. Primordia were imaged once per hour as stacks of 150 images at 0.5 μm z-spacing.

during LRP development and several patterns of cell division converge onto the same morphological structure.

LRP Shape but Not the Pattern of Cell Division Is Highly Constrained During Organogenesis.

Following our observation that the pattern of cell divisions is variable in LRPs, we investigated its impact on organ shape. We performed statistical shape analysis on LRPs using the same z-stack confocal database used to monitor LRP cell numbers. The outer structure of a LRP was defined as a Bezier curve with 26 control points (Fig. 3A) that outlined the shape of the LRP observed in its previously defined median plane (Fig. 3B). The outermost pair of points on each side of the LRP corresponded to the corners of the flanking cells as defined by pAUX1:AUX1-YFP primordium expression. The remaining points were chosen to be equally spaced along the LRP. We used these 26 control points as “landmarks” to perform statistical shape analysis.

For each stage of primordium development, we carried out Generalized Procrustes Analysis (GPA) of all of the LRP shapes at that stage (16) (Fig. 3C). This involves translating, rotating, and scaling the shapes to minimize the sum of squared error (*Materials and Methods*). We found that for a given stage, LRP profiles appeared homogeneous (Fig. 3C). To quantify the profile similarity between different LRPs, we calculated the distances of the shapes

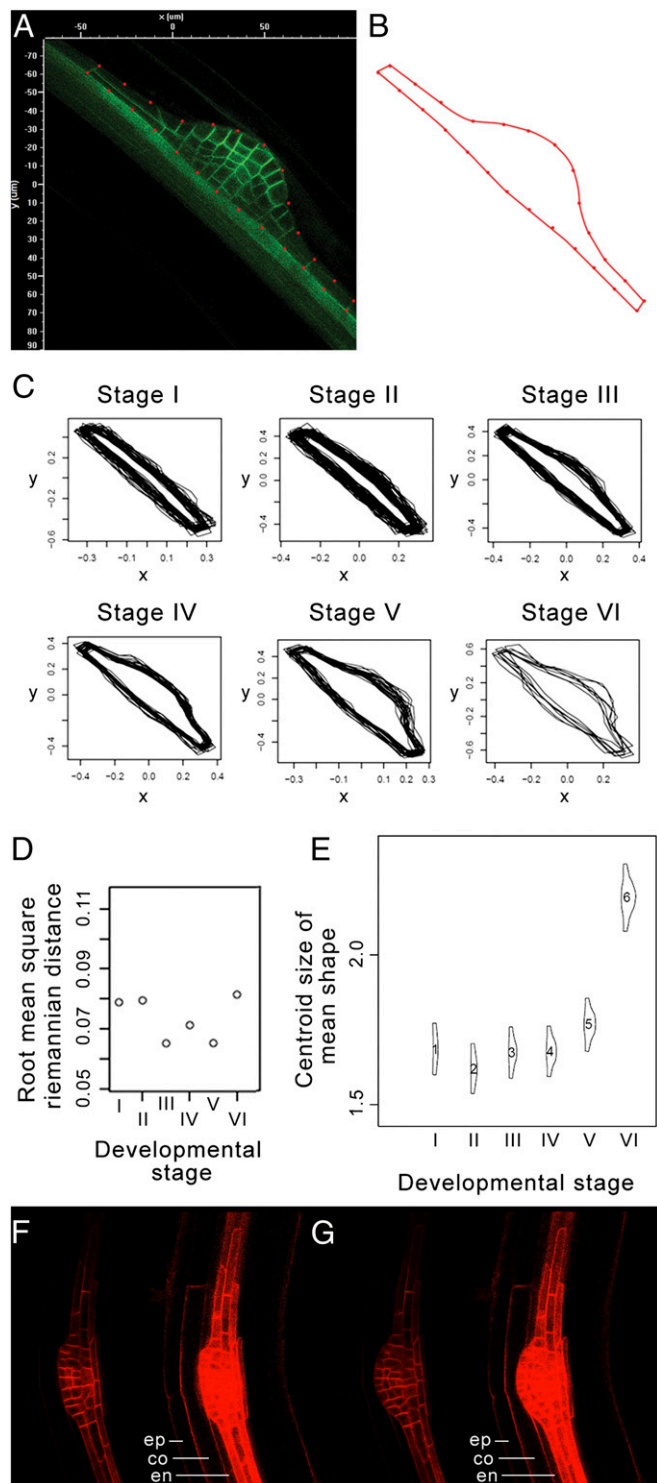


Fig. 3. LRP shape is highly regular. (A and B) The external shape of LRPs that express pAUX1:AUX1-YFP was extracted from the median optical slice of confocal z-stacks. For each LRP, 26 control points were used to define the 2D shape. (C) GPA of LRP shapes at each developmental stage ($n = 194$). (D) Root mean square distance between LRP shapes and the mean shape at each stage. (E) Centroid size of LRP mean shape at each stage. (F and G) Observation of a LRP induced by gravistimulation in the pAUX1:AUX1-YFP transgene line at 16 h (F) and 18 h (G) after gravistimulation. The left sides of the panels show only the LRP structure, and the right sides correspond to the same images at a higher saturation level, highlighting the outer tissue structure on top of the LRP (due to low-level pAUX1:AUX1-YFP expression). co, cortex; en, endodermis; ep, epidermis. Primordium was imaged as a stack of 300 images at 0.5 μm

at a particular stage from the “mean shape” at that stage. The root mean square distance is analogous to the SD as a measure of the variability of the distances from the mean shape at a given stage. The root mean square distance values at each of the different stages were found to be very low (Fig. 3D), demonstrating that LRP outer shape is conserved for a given developmental stage.

We estimated the centroid size of the “mean shape” at each stage and found that significant shape size changes occurred at the transition between stages IV and V/VI (Fig. 3E). Analysis of confocal time series of pAUX1:AUX1-YFP-expressing LRPs revealed that this transition corresponds to a drastic shape change between “flat-topped” (Fig. 3F) and “dome-shaped” (Fig. 3G) as the LRP breaks through the endodermis. This shape transition occurs in less than 2 h and is not related to an increase in cell proliferation at that stage (Fig. 2C and Fig. S4). Instead, this LRP shape transition is most likely due to structural constraint relaxation after the Casparian strip breaks (Movie S4). Indeed, a high time resolution movie (down to every 7.5 min) detected the LRP rupturing the endodermis within minutes, causing the primordium to appear to “jump” (Movie S5). The Casparian strip is a lignified net-like structure that cements endodermal cells together to form an impermeable barrier (17, 18) through which LRPs are required to pass to emerge into the soil environment. To test this hypothesis, we analyzed LRP development in the enhanced *suberin1* (*esb1-1*) (19) and *casparian strip membrane domain protein* (*caspl-1*)/*caspl-3-1* (17) mutants. *esb1-1* mutants present an increase in suberin deposition in the entire endodermis cell wall, while *caspl-1/caspl-3-1* mutants exhibit deposit of Casparian strip material in the entire anticlinal endodermis cell wall rather than in a tight band on this wall. In agreement with our hypothesis, we observed an increase in LRP flattening in these mutants (Fig. S5A) and a delay in their emergence, resulting in lower emerged lateral root densities (Fig. S5B and C). Fine analysis of LRP emergence kinematics using gravistimulation to synchronize LRP development revealed that *esb1-1* LRPs are delayed in early emergence, while *caspl-1/caspl-3-1* LRPs are delayed in mid- to late emergence (Fig. S5D and E). Together these results indicate that the Casparian strip creates a biomechanical constraint influencing the LRP morphogenesis and emergence.

The rapid shape transition observed is only possible if the LRP is under internal pressure when the endodermis/Casparian strip finally breaks. Analysis of our image database revealed that the cell division rate in LRP is the same when first starting to push through the endodermis until it ruptures, and afterward while passing through the cortex (Fig. S6). Our results therefore suggest that the internal pressure of the LRP would rise through cell accumulation as it pushes against the endodermis. While LRPs exhibit significant variability in cellular organization for a given stage, organ shape is highly conserved at each stage, and a major shape change is associated with the breaking of the endodermis-casparian strip barrier. Hence, our data indicate that LRP shape might be more influenced by the mechanical constraints imposed by the overlying tissues rather than the exact pattern of cell divisions.

Overlying Tissues Rather than Cell Division Pattern Impacts LRP Shape. To probe the relative importance of patterns of cell division and overlying tissues on LRP morphogenesis, we used a variety of genetic and transgenic approaches. We initially assessed the impact of disrupting the organized pattern of cell divisions on LRP shape. This was performed by analyzing the *aurora 1 aurora 2* (*aur1-2;2-2*) double mutant lacking key AURORA kinases that are required to correctly position the cell

z-spacing. Observation of a LRP induced by gravistimulation in the pAUX1:AUX1-YFP transgene line at 16 h (F) and 18 h (G) after gravistimulation. The left sides of the panels show only the LRP structure, and the right sides correspond to the same images at a higher saturation level, highlighting the outer tissue structure on top of the LRP (due to low-level pAUX1:AUX1-YFP expression). co, cortex; en, endodermis; ep, epidermis. Primordium was imaged as a stack of 300 images at 0.5 μm z-spacing.

plate in LRPs following mitosis (20). This results in a chaotic pattern of cell plate deposition in LRPs (Fig. 4A and Fig. S7A). Despite this major disruption to the organized pattern of cell division, statistical shape analysis revealed that LRP morphogenesis in *aur1-2;2-2* produces normal-shaped primordia (Fig. 4 and Fig. S8). Our observations using the *aur1-2;2-2* mutant thus imply that the pattern of cell divisions does not play a major role in the global LRP shape. We additionally investigated the impact of the *aur1-2;2-2* mutation on primordia 3D morphogenesis using light-sheet microscopy. We first analyzed the growth dynamics of the *aur1-2;2-2* mutant. Whereas the wild-type LRP grows monotonously, the mutant had a “stop and go” profile (Fig. 4B and Movie S6). In addition, the progressive radialization observed in the wild type LRPs was replaced by an erratic decrease in the *aur1-2;2-2* mutant (Fig. 4C and D), and we observed that radial and tangential divisions were not restricted to the daughter cells flanking the central file (Fig. S7B). Taken together, these findings suggest that while cell division patterns are not responsible for global LRP shape, LRP cellular organization contributes to the definition of LRP potential growth axis.

We next tested the impact of altering the mechanical properties of the tissues overlaying new LRPs to assess their effect on organ shape. Auxin originating from LRPs has been described to trigger a cascade of signaling events in overlaying cells, culminating in the induction of several cell wall remodeling enzymes that alter their mechanical properties (21). To block auxin responses in root cells overlaying new LRPs in an inducible manner, we have developed a steroid-regulated system that provides both spatial and temporal regulation. Our system employs a glucocorticoid receptor (GR) sequence fused in frame to the stabilized auxin transcriptional repressor IAA17/AXR3. This *axr3-1-GR* sequence is fused downstream of the UAS regulatory sequence, so that transgene expression can be targeted to selected tissues in a GAL4-

dependent manner. The GAL4 driver line J0631 expressed in all cell layers of the root but not in the meristem or LRP (Fig. S9) was used for transactivation of *UAS::axr3-1-GR* to selectively block auxin responses in a steroid- (Dexamethasone, DEX) inducible manner in non-LRP tissues. In the absence of DEX, J0631>>*axr3-1-GR* seedlings continued to form normal-shaped primordia (Fig. 4A). In contrast, in the presence of DEX, J0631>>*axr3-1* roots failed to form normal-shaped primordia (Fig. 4A and Fig. S8). Primordia development also appeared greatly delayed in the presence of DEX (Fig. S10). We conclude that disrupting the pattern of cell divisions does not impact LRP shape, but manipulating the properties of overlaying tissues disrupted LRP morphogenesis.

Conclusion

Arabidopsis lateral root development has represented a model system to study root morphogenesis for the last two decades, yet our understanding has remained essentially 2D (7). Recent advances in live biological imaging and image analysis (8, 9) now make it possible to address how plant organs are built in three and four dimensions. LRP morphogenesis is characterized by a transition from bilateral to radial symmetry that reflects the origin of primordia founder cells from a limited starting cell pool (i.e., three pairs of xylem-pole pericycle cells). We observed that daughter cells derived from the flanking pairs of pericycle cells exhibit atypical tangential or radial cell divisions during LRP morphogenesis. These tangential and radial cell divisions play a critical role in the transition from bilateral to radial symmetry. Moreover, the ring of cells created by these tangential and radial divisions is likely to perform a buttress-like function for the population of rapidly proliferating inner cells that form the LRP apex (12). It will be interesting to identify the molecular

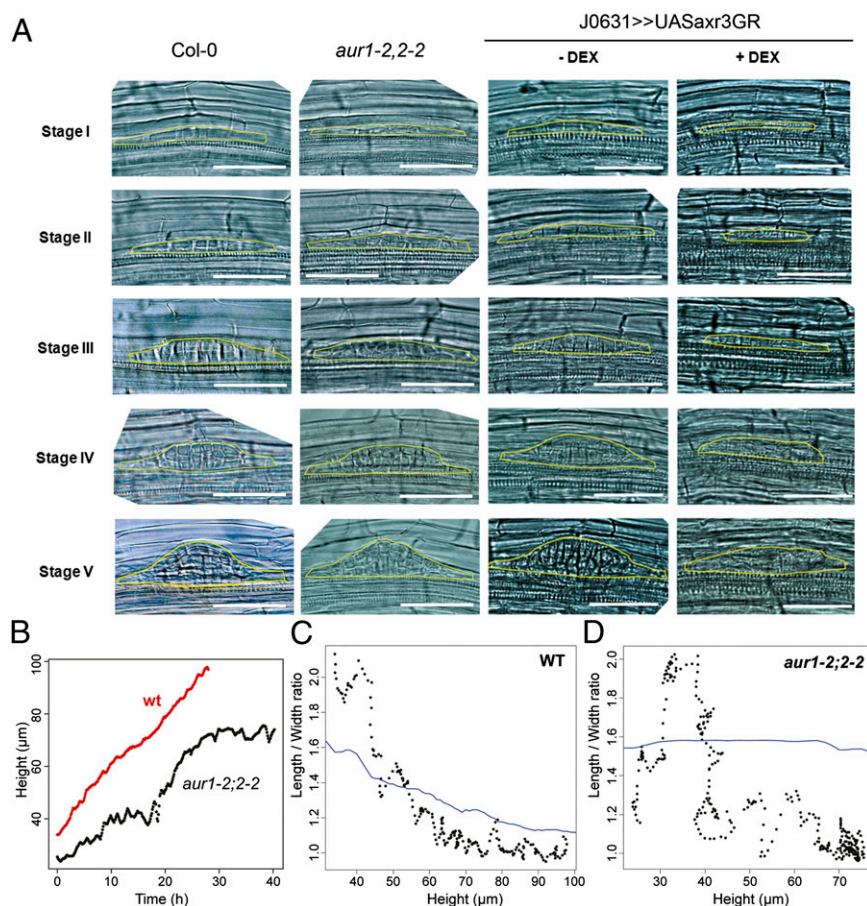


Fig. 4. Overlaying tissues rather than cell division pattern canalize LRP shape. (A) Impact of *aur1-2;2-2* double mutation or outer tissue-targeted *axr3* expression on primordia shape development. LRP shapes are outlined in yellow. (B) Growth dynamics of primordia in *aur1-2;2-2* double mutant. Wild-type and *aur1-2;2-2* double mutant expressing the pPIN1::PIN1-GFP construct LRP were imaged in light-sheet microscopy. (C and D) L-W ratio as a function of LRP height for wild-type (C) and *aur1-2;2-2* double mutant (D) primordia. The ratio was measured as described in Fig. 1D. The blue line is a Lowess fit.

mechanism(s) responsible for this type of cell division as recently described for root periclinal cell divisions (22). The net result of these tangential and radial divisions is to create an ellipsoid-shaped LRP. From a functional point of view, an ellipsoid-shaped LRP would facilitate organ emergence through the outer tissue layers.

Live imaging also revealed that the precise pattern of cell divisions during *Arabidopsis* LRP morphogenesis is variable. LRPs passing through the same developmental stage contain markedly different numbers of cells. Although the total number of cells in LRPs can vary greatly for a given stage, the global rate of cell division is constant throughout LRP morphogenesis. This most likely reflects that LRPs contain variable numbers of rapidly proliferating inner cells that fill the central space created by the ring of cells created by tangential divisions. Hence, there appears to be no unique sequence of formative cell divisions during LRP development, giving rise to the multicellular structure. Indeed, we demonstrated that disrupting the pattern of cell divisions using the *aur1 aur2* double mutant had only a minor effect on LRP shape.

We also report that the development of LRP shape is highly canalized and primarily results from the mechanical constraints of overlaying tissues rather than the pattern of cell divisions. Using casparian strip mutants as well as targeted alteration of the overlaying tissue auxin response and mechanical properties, we show that the LRP shape can be modified. We additionally showed that while the precise cellular patterning of LRP is not responsible for LRP shape, it conditions the potential axis of growth of the LRP. This finding emphasizes the importance of coordinated processes between the developing LRP and its surrounding tissue for proper emergence.

Recent studies have highlighted the importance of the localized auxin signal originating from the tip of the LRP to induce specific physiological responses in overlaying tissues (22, 23). Biomechanical properties targeted by auxin include production of cell wall remodeling enzymes (21) through the IDA-HAE/HSL2 signalling pathway (24, 25) and down-regulation of water channels termed aquaporins to alter hydraulic properties of overlaying tissues (23). Mutants lacking these auxin targets exhibit altered LRP shape (23). LRP morphogenesis therefore appears to be “canalized” from mechanical feedback between the new organ and overlaying tissues. We hypothesize that such a regulatory arrangement would serve to optimize the process of organ emergence through overlaying tissues to minimize damage and thereby help limit the potential for infection by pathogenic soil microorganisms.

Materials and Methods

Plant Lines and Growth Conditions. Seeds were surface-sterilized for 8 min in 50% (vol/vol) bleach and then washed twice in 0.1% (vol/vol) triton X-100. Seeds were then plated on square plates containing 0.5× Murashige and Skoog (MS) salt mixture and 1% (wt/vol) bacto agar. Plates were cold treated for 2 d at 4 °C in the dark to synchronize germination. Plates were then incubated in a near-vertical position at 23 °C in 150 μmol photons·m⁻²·sec⁻¹ with a cycle of 18 h light/6 h dark. The *aur1-2;2-2-pPIN1::PIN1-GFP* transgenic and mutant lines were described previously (20). Details about constructions of the other lines can be found in *SI Materials and Methods*.

Targeted Transactivation. We transferred 3-d-old seedlings onto media containing 10 μM DEX or no DEX, and lateral roots were profiled in optical microscopy on the fifth day following transfer.

Microscopy and LRP Observation. LRPs were imaged as z-stacks in confocal microscopy using either a Nikon Eclipse C1 or Leica SP5 as described previously (26). Images were taken with a Plan Fluor 20.0×/0.50 lens (Fig. 1 A and B) or with a Plan Fluor 40.0×/0.75 lens (Figs. 1F, 2 A and D, and 3 F and G). The medium plane of the z-stack corresponding to the central plane of the developing LRP was used as a reference image for the structural analyses. LRP 2D shapes used for statistical analysis were defined by Bezier curves using 26 control points per primordium. Light-sheet microscopy was performed as described previously (9). Images were taken with either a Carl Zeiss W N-Achroplan 20×/0.5 (Fig. 1D) or 40×/0.75W (Fig. 1C) objective lens for the detection and a Carl Zeiss EC Plan-Neofluar 5×/0.16 objective lens for illumination.

Image Processing and Analysis. All postacquisition image processing was performed using Fiji, AMIRA, and OpenAlea (27). More details on statistical shape analysis and measurements of LRP radialization can be found in *SI Materials and Methods*. Statistical analysis and graphing was performed in R (28).

ACKNOWLEDGMENTS. This work was supported by the Biotechnology and Biological Sciences Research Council (BBSRC) and Engineering and Physical Sciences Research Council funding to the Centre for Plant Integrative Biology, a “Chercheur d’Avenir” grant from the Région Languedoc-Roussillon (to M.L., S.G., and L.L.), the Institut de Recherche pour le Développement (to L.L.), Université Montpellier 2 (to S.G. and L.L.), an Agropolis Fondation “Rhizopolis” Federative Grant (to M.L., C.G., S.G., and L.L.) Land Baden-Württemberg, the Chica and Heinz Schaller Stiftung and the CellNetworks cluster of excellence (to A.M.), the Cluster of Excellence “Macromolecular Complexes” at the Goethe University Frankfurt (DFG Project EXC 115) (to D.v.W. and E.H.K.S.), a BBSRC David Phillips Fellowship and a Marie Curie European Reintegration Grant (to I.D.S.), and a postdoctoral fellowship from the Research Foundation—Flanders (to D.V.D.).

- De Smet I, Vanneste S, Inzé D, Beeckman T (2006) Lateral root initiation or the birth of a new meristem. *Plant Mol Biol* 60(6):871–887.
- De Smet I (2012) Lateral root initiation: One step at a time. *New Phytol* 193(4):867–873.
- Kennaway R, Coen E, Green A, Bangham A (2011) Generation of diverse biological forms through combinatorial interactions between tissue polarity and growth. *PLOS Comput Biol* 7(6):e1002071.
- Robinson S, et al. (2011) Generation of spatial patterns through cell polarity switching. *Science* 333(6048):1436–1440.
- De Smet I, Lau S, Mayer U, Jürgens G (2010) Embryogenesis—The humble beginnings of plant life. *Plant J* 61(6):959–970.
- Péret B, et al. (2009) Arabidopsis lateral root development: An emerging story. *Trends Plant Sci* 14(7):399–408.
- Malamy JE, Benfey PN (1997) Organization and cell differentiation in lateral roots of *Arabidopsis thaliana*. *Development* 124(1):33–44.
- Fernandez R, et al. (2010) Imaging plant growth in 4D: Robust tissue reconstruction and lineaging at cell resolution. *Nat Methods* 7(7):547–553.
- Maizel A, von Wangenheim D, Federici F, Haseloff J, Stelzer EHK (2011) High-resolution live imaging of plant growth in near physiological bright conditions using light sheet fluorescence microscopy. *Plant J* 68(2):377–385.
- Laplace L, et al. (2005) GAL4-GFP enhancer trap lines for genetic manipulation of lateral root development in *Arabidopsis thaliana*. *J Exp Bot* 56(419):2433–2442.
- De Smet I, et al. (2008) Receptor-like kinase ACR4 restricts formative cell divisions in the Arabidopsis root. *Science* 322(5901):594–597.
- Kurup S, et al. (2005) Marking cell lineages in living tissues. *Plant J* 42(3):444–453.
- Swarup R, et al. (2004) Structure-function analysis of the presumptive Arabidopsis auxin permease AUX1. *Plant Cell* 16(11):3069–3083.
- Geldner N, et al. (2009) Rapid, combinatorial analysis of membrane compartments in intact plants with a multicolor marker set. *Plant J* 59(1):169–178.
- Benková E, et al. (2003) Local, efflux-dependent auxin gradients as a common module for plant organ formation. *Cell* 115(5):591–602.
- Dryden IL, Mardia KV (1998) *Statistical Shape Analysis* (Wiley, New York).
- Roppolo D, et al. (2011) A novel protein family mediates Casparian strip formation in the endodermis. *Nature* 473(7347):380–383.
- Naseer S, et al. (2012) Casparian strip diffusion barrier in Arabidopsis is made of a lignin polymer without suberin. *Proc Natl Acad Sci USA* 109(25):10101–10106.
- Ranathunge K, Schreiber L (2011) Water and solute permeabilities of Arabidopsis roots in relation to the amount and composition of aliphatic suberin. *J Exp Bot* 62(6):1961–1974.
- Van Damme D, et al. (2011) Arabidopsis α Aurora kinases function in formative cell division plane orientation. *Plant Cell* 23(11):4013–4024.
- Swarup K, et al. (2008) The auxin influx carrier LAX3 promotes lateral root emergence. *Nat Cell Biol* 10(8):946–954.
- Dhonukshe P, et al. (2012) A PLETHORA-auxin transcription module controls cell division plane rotation through MAP65 and CLASP. *Cell* 149(2):383–396.
- Péret B, et al. (2012) Auxin regulates aquaporin function to facilitate lateral root emergence. *Nat Cell Biol* 14(10):991–998.
- Stenvik GE, et al. (2008) The EPIP peptide of INFLORESCENCE DEFICIENT IN ABSCISSION is sufficient to induce abscission in Arabidopsis through the receptor-like kinases HAESA and HAESA-LIKE2. *Plant Cell* 20:1805–1817.
- Kumpf RP, et al. (2013) Floral organ abscission peptide IDA and its HAE/HSL2 receptors control cell separation during lateral root emergence. *Proc Natl Acad Sci USA* 110:5235–5240.
- Lucas M, et al. (2011) Short-Root regulates primary, lateral, and adventitious root development in Arabidopsis. *Plant Physiol* 155(1):384–398.
- Pradal C, Dufour-Kowalski S, Boudon F, Fournier C, Godin C (2008) OpenAlea: A visual programming and component-based software platform for plant modelling. *Funct Plant Biol* 35(10):751–760.
- R Development Core Team (2011) *R: A language and environment for statistical computing*. R Foundation for Statistical Computing, Vienna, Austria. ISBN 3-900051-07-0, <http://www.R-project.org/>.